Check for
updates

The Invariance of the Tisserand Parameter in Various Gravitational Theories

Ioannis Haranas[1] · Youssef M. Shehata[2] · Kristin Cobbett[2] · Ioannis Gkigkitzis[3] · Dimitrios Theodore Kalafatis[4] · Ryan Gauthier[2]

Abstract

In today's gravity research there exists a number of gravitational theories which predict the existence of various corrections to the classical gravitational potential. In this paper using the different potentials that exist in the literature and with the help of Gauss' planetary equations we examine the time rate of change of the Tisserand parameter as a function of the time rate of change of the three orbital elements involved. We find that the Tisserand parameter remains constant over a full orbital revolution in all the different potential resulting from the various theories. This fortifies and generalises the use of Tisserand parameter not only in case of Newtonian dynamics but also in more extended theories of gravity, thus ensuring its validity in determining the identity of a returning comet. Furthermore, we find that the parameter remains unchanged even in the case where a gravitational potential derived from a D-dimensional gravitational force, in the case where $D = 4$. Next quantization of orbits calculation is performed and the constancy of the Tisserand parameter is also recovered. Finally, assuming fractal orbits we obtain an expression for the fractal dimension of three well known Jupiter family comets in terms of their orbital elements and the constancy of the Tisserand parameter is also recovered.

Keywords Tisserand parameter · Jupiter family comets · Gauss planetary equations · Gravity theories · Fractals

1 Introduction

Comets that move in elliptical orbits periodically appear in the vicinity of the solar system. For these types of comets their eccentricities and semi-major axes are usually large. As a result, their periodic orbits carry them away in the far ends of the solar system. Under these conditions no comet can be really followed visually all the way as planets do in their orbits. To follow a comet in every point of its orbit it's not an easy task. In the the appearance of a new comet, it is always hard to identify the comet with an old periodic one. In other words, the identification of an old comet with a new one is always a problem.

The simplest method consists in the comparison of the comet's previous orbital elements with the orbital elements of the newly discovered comet. But this method it's not

---

always acceptable since comets travelling in elliptical orbits pass near the large planets such as Jupiter, can suffer gravitational perturbations that can significantly change their orbit from elliptic to parabolic or vice versa (Gurzadyan 1996). Because comets can suffer greatly at any perihelion passage their physical characteristics can be significantly altered, therefore their natural appearance cannot be really preserved on the cosmological time scale as the appearance of the planets, with solar radiation pressure to be one of the most important perturbations. The action of energetic photons emanating from the sun along with elementary particles can significantly change the comet's physical appearance. For example, cometary characteristics that can change is brightness, the size of the core, or the tail, and as a result the identification of the comet based on these it's not possible.

A method often used is the computation of the orbital elements of the initial comet considering all possible perturbation and the comparison with the orbital elements of the new comet. However, this is a very long and time-consuming method and therefore some other method or probably a new criterion would be more suitable for reaching such a conclusion. We say that such a criterion exists, and it is called Tisserand's criterion. It involves a combination of the orbital elements semimajor axis a, eccentricity e, and inclination i and the function $\Phi(a, e, i) = C_0$ composed from these orbital elements and preserves its constancy regardless of any perturbations acting on the comet's orbit. Furthermore, for such a combination it's always true that $\Phi(a_0, e_0, i_0) = \Phi(a_1, e_1, i_1) = C_0$ a relation that is also satisfied during all the appearances of the orbiting comet. A violation of this criterion would imply that the new comet is a different one.

Next, let us suppose that a comet is to be observed before and after its close approach to Jupiter. Let us assume that a_0, e_0, i_0 and a_1, e_1, i_1 refer to the orbital elements of the old and new orbit. Therefore following (Bertotti et al. 2003) we can write Tisserand's criterion in the following way:

$$\frac{1}{a_0} + 2\cos i\sqrt{a_0\left(1 - e_0^2\right)} = \frac{1}{a_1} + 2\cos i_1 \sqrt{a_1\left(1 - e_1^2\right)} = C_0 \tag{1}$$

This is the mathematical formula for Tisserand's criterion. Furthermore, following (Bertotti et al. 2003) and for a comet in a frame rotating with Jupiter's, we can write Tisserand's criterion in slightly different way (ibid 2003):

$$T = \frac{a_J}{a} + 2\cos i\sqrt{\frac{a}{a_J}\left(1 - e^2\right)} = -\frac{2a_J}{GM}\left(\frac{Gm}{r_2} + C\right) \tag{2}$$

where a_J is the semimajor axis of Jupiter, a is the semimajor axis of the comet, e it's eccentricity and i is its inclination with respect to Jupiter's orbital plane, and r_2 is the distance of the comet from Jupiter, and m its mass. Therefore, in two different apparitions the comet is far enough from Jupiter, the expression in the left-hand side of Eq. (2) has to approximately have the same value, regardless of any close approach to Jupiter that has already occurred in the meantime which has altered the orbital elements. The constancy of Tisserand's invariant is very useful in the restricted 3Body treatment whenever it requires some constraint on the orbital changes that might result to a close encounters. In an early paper by Carusi et al. (1995) the authors check the conservation of various formulations of the Tisserand parameter and investigate the relations between T-values and the dynamical behaviours at close encounters with Jupiter. Next, in Bottke et al. (2002) the authors investigate the orbital and absolute magnitude distribution of the near-Earth objects (NEOs), something that is difficult to compute partly because only a modest fraction of the entire NEO population has been discovered so far, but also because the known NEOs are biased by

complicated observational charactetristics. Similarly, in Angor and Lin (2011) the authors examine how the late divergent migration of Jupiter and Saturn may have perturbed the terrestrial planets. The authors identify six secular resonances between the apsidal eigenfrequency of Jupiter and Saturn and the four eigenfrequencies of the terrestrial planets to values larger that the observed ones. Finally, in a recent paper by Hsieh and Haghighipour (2016) the authors present the results of "snapshot" numerical integrations of test particles representing comet-like and asteroid-like objects in the inner solar system, aimed at investigating the short-term dynamical evolution of objects close to the dynamical boundary between asteroids and comets as defined by the Tisserand parameter with respect to Jupiter, T_J (i.e., $T_J = 3$). More recently data and analysis various interferometric gravitational wave detectors is already on the way. The goal of the scientific community aimed for the detection of gravitational waves (Corda 2009). There is no doubt that such a detector can and will open a new window in the observation of the universe also confirm or rule out the theory of general relativity as well as any other know theories of gravitation. (Corda 2008)

In this paper, the constancy of the Tisserand parameter is examined for several different gravitational potentials, resulting in various gravity theories in a two-body orbital scenario including also the case of a dimensionality $D = 4$ space gravitational force. Furthermore, using three well known Jupiter family comets we attempt the examination of the Tisserand parameter in the case where the cometary orbits can be represented as fractal orbits of a fractal dimension that is expressed as a function of orbital elements. Concluding, we say the main idea of this contribution is the examination of any possible deviations on cometary Tisserand parameter in gravitational potential derived from various gravitational theories if any.

2 The Logarithmic Potential

Four fundamental forces govern the universe, one of which is gravity, long known to be an inverse square field. On the other hand, Einstein's theory of gravitation is a more complete theory where gravitation is related to the space–time curvature of the universe. Having said that today's scientists know that Einstein's theory help us to understand the nature of astronomical and astrophysical phenomena, where at the same time the theory fails in understanding and explain certain types. For recent critical overviews of general relativity (GR) look Iorio, (2015). One of the major difficulties that the theory of gravitation faces, is that of the flat rotation curves in spiral galaxies. As an explanation today's science has postulated the idea of dark matter which mathematically enters as a gravitational potential modification in the weak field approximation. The assumption is that dark matter is made up of non-baryonic matter which populates the galactic halos of various galaxies, with dark matter distributions above the galactic plane of our Galaxy and other spiral galaxies. The first evidence of dark matter was first found by Zwicky in 1937 (Binney and Tremaine 1987). Zwicky's work was based on radial velocity measurements of galaxies belonging to the Coma cluster (ibid 1987). In the limit of the very weak field approximation dark matter is treated as a modification of the gravitational potential, in which case Modified Newtonian Dynamics (MOND) was first proposed by Milgrom (1983). In his theory Milgrom postulates that Newtonian gravitational force is strengthened for the accelerations within the range that is below the usual Newtonian gravitational force. He further gives an empirical value for this acceleration that is approximately equal to $a_0 \sim 1.2 \times 10^{-10}$ m/s². In another paper Sanders and Noordermeer (2007) indicate that this acceleration is adequate

when applied to the galactic rotation curves. Finally, in a paper by Haranas et al. (2020) the authors study the motion of a secondary celestial body under the influence of a corrected gravitational potential in a modified Newtonian dynamics scenario. Specifically, the authors examine in orbits within the Milky-Way galaxy, where the application of a modified Poisson equation results into two new potential terms one of which is logarithmic and the other involves the cosmological constant lambda Λ which in the region of influence of the logarithmic correction to the potential is related to the condition, $r > r_{max}$ the logarithmic correction is also related to the term $(\nabla\phi)^2$ in the modified Poisson equation for the gravitational field (ibid 2020).

3 Rate of Change and Variation of the Tisserand Parameter

Let us now consider a Jupiter family comet, orbiting around the Sun with aphelion in the vicinity of Jupiter in an elliptical orbit. Let a be the semimajor axis, e its eccentricity, and i its inclination with respect to Jupiter's orbital plane. Using Eq. (2) and, taking the derivative of T_c we obtain the following expression:

$$\frac{dT_c}{dt} = \left(-\frac{a_J}{a^2} + \cos i \sqrt{\frac{(1-e^2)}{a_J a}}\right)\frac{da}{dt} - \frac{2ea\cos i}{\sqrt{a_J a(1-e^2)}}\frac{de}{dt} - 2\sin i\sqrt{\frac{a(1-e^2)}{a_J}}\frac{di}{dt} \quad (3)$$

Next, following Haranas et al., (2015) from Gauss' equations for da/dt we have that:

$$\frac{da}{dt} = \frac{2}{n\sqrt{1-e^2}}\left[eR\sin f + \frac{a(1-e^2)}{r}T\right] \quad (4)$$

where R and T are the radial and transverse components of this acceleration per unit mass, and f is the true anomaly, a the semimajor axis, and e is the eccentricity and n is the mean anomaly of the comet. Similarly, following Vallado (2001) we write that:

$$\frac{de}{dt} = \frac{\sqrt{1-e^2}}{na}\left[R\sin f + T(\cos f + \cos E)\right] \quad (5)$$

$$\frac{di}{dt} = \frac{r\cos(\omega+f)}{na^2\sqrt{1-e^2}}W \quad (6)$$

Since logarithmic field is a radial field, the radial acceleration R_{log} is the only not zero acceleration along the radial direction, such that T and $W=0$ therefore Eqs. (4), (5), (6) become:

$$\frac{da}{dt} = \frac{2eR_{log}\sin f}{n\sqrt{1-e^2}} \quad (7)$$

$$\frac{de}{dt} = \frac{\sqrt{1-e^2}}{na}R_{log}\sin f \quad (8)$$

$$\frac{\mathrm{d}i}{\mathrm{d}t} = 0 \tag{9}$$

Using Eqs. (7), (8), (9) Eq. (3) can be written as:

$$\frac{\mathrm{d}T_c}{\mathrm{d}t} = \left(\frac{a_J}{a^2} + \cos i \sqrt{\frac{(1-e^2)}{a_J a}} \right) \left(\frac{2eR_{\log} \sin f}{n\sqrt{1-e^2}} \right) - \frac{2ea\cos i}{\sqrt{a_J a (1-e^2)}} \left(\frac{R_{\log} \sin f \sqrt{1-e^2}}{na} \right) \tag{10}$$

Next, the radial component of the logarithmic acceleration is given by the equation (Haranas et al. 2020):

$$R_{\log} = -\frac{\partial V}{\partial r} = -\frac{\partial}{\partial r}\left(-\alpha GMm \ln\left(\frac{r}{r_0} \right) \right) = \frac{\alpha GM}{r} \tag{11}$$

Next, we express the time rate of change of the Tisserand parameter (10) in terms of the eccentric anomaly E by using the well-known relations (Murray and Dermott 1999):

$$r = a(1 - e \cos E), \tag{12}$$

$$\frac{dE}{dt} = \frac{n}{1 - e\cos E} \tag{13}$$

$$\sin f = \frac{\sqrt{1-e^2}\sin E}{(1 - e\cos E)} \tag{14}$$

Substituting Eqs. (12) into (11) we obtain that:

$$R_{\log} = \frac{\alpha GM}{a(1 - e \cos E)} \tag{15}$$

Next using (13) and (14) Eq. (10) takes the form:

$$\frac{\mathrm{d}T_c}{\mathrm{d}E} = \frac{(1 - e\cos E)}{n} \left[A_o \left(\frac{2e}{n\sqrt{1-e^2}} \frac{\sin E\sqrt{1-e^2}}{(1-\cos E)} \frac{\alpha GM}{a(1-e\cos E)} \right) - B_0 \left(\frac{\sin E\sqrt{1-e^2}\sqrt{1-e^2}}{na(1-\cos E)} \frac{\alpha GM}{a(1-e\cos E)} \right) \right], \tag{16}$$

where:

$$A_0 = \left(\frac{a_J}{a^2} + \cos i \sqrt{\frac{(1-e^2)}{a_J a}} \right), \tag{17}$$

$$B_0 = \frac{2ea\cos i}{\sqrt{a_J a (1-e^2)}} \tag{18}$$

And Eq. (16) can be simplified as follows:

$$\frac{\mathrm{d}T_c}{\mathrm{d}E} = \left[A_o \left(\frac{2e\alpha GM}{na} \frac{\sin E}{(1 - e\cos E)} \right) - B_0 \left(\frac{\alpha GM(1 - e^2)\sin E}{na^2(1 - e\cos E)} \right) \right], \quad (19)$$

Integrating over a full revolution

$$T_{final} = T_{init} + \int_0^{2\pi} \left[A_o \left(\frac{2e\alpha GM}{na} \frac{\sin E}{(1 - \cos E)} \right) - B_0 \left(\frac{\alpha GM(1 - e^2)\sin E}{na^2(1 - \cos E)} \right) \right] \mathrm{d}E \quad (20)$$

To integrate

$$\int_0^{2\pi} \frac{\sin E}{(1 - e\cos E)} \mathrm{d}E, \quad (21)$$

we use substitution letting $(1\text{-}e\cos E) = u$ the integral becomes:

$$\frac{1}{e} \int_{1-e}^{1-e} \frac{du}{u} = 0 \quad (22)$$

and therefore, by a basic rule of the definite integrals, we obtain that:

$$T_{final} = T_{init} = \text{constant} \quad (23)$$

Therefore, in the case of a logarithmic potential the Tisserand parameter remains constant.

4 The Yukawa Potential

The force of gravitation is one of the four fundamental forces of nature. When compared to electromagnetic, strong and weak forces, gravitation still resists a quantum mechanical explanation that involves the exchange of some kind of bosons. In spite the fact that various theoretical models have proposed, its unification with the rest of the physical forces still remains impossible. Deviations from the Newtonian gravitational potential can be described with an additional Yukawa correction (Fischbach et al. 1986, 1992).

The effects of gravity on the secondary in the presence of the Yukawa correction can be described in terms of the modified potential (Haranas et al., 2010):

$$V(r) = -\frac{GM_p}{r} \left(1 + \alpha e^{-\frac{r}{\lambda}} \right) \quad (24)$$

In this relation, r denotes the distance between the two bodies, G is the Newtonian gravitational constant, $\alpha = kK/GMm$, where k and K are the coupling constants of the new force to the bodies relative to the gravitational one (Iorio 2002), and λ is the range the mediating the interaction particle (Haranas et al. 2010). The corresponding force per unit mass can be written as:

$$F(r) = -\frac{GM_p}{r^2}\left[1 + \alpha\left(1 + \frac{r}{\lambda}\right)e^{-\frac{r}{\lambda}}\right]\hat{r} = R_{Yuk} \tag{25}$$

Kolosnitsyn and Melnikov (2004) have calculated that for the artificial Earth satellites LAGEOS and LAGEOS II, a minimum value of the Yukawa coupling constant is of the order of $\alpha_{min} = 1.38 \times 10^{-11}$ for $\lambda = 6.081 \times 10^6$ m. Haranas et al. (2010). We have also mention that in earlier papers by Iorio (2002) and Lucchesi (2003), the authors dealt with the perigee motion rate for the same LAGEOS satellites. Moreover, Pitjeva (1999) has estimated using radar measurements that random Mercury perihelion motions are of order 0.052 arcsec/cycle, which implies that, $\alpha_{min} = 3.57 \times 10^{-10}$ for $\lambda = 2.89 \times 10^{10}$ m. She extended such research to other solar-system bodies, also tackling the problem of the solar-system dark matter and its influence on other planets dynamics (Pitjeva 2009). In connection with Pitjeva's results, we must quote Iorio's (2007) paper, which put severe constraints on λ, showing that the range cannot exceed 1 AU. This finding may have important consequences on all gravity theories that involve Yukawa-type corrections with range parameters much larger than the solar-system size. Next, the radial component of the Yukawa acceleration is given by the equation (Haranas et al. 2010):

$$R_{Yu} = -\frac{GM_p\alpha}{r^2}\left(1 + \frac{r}{\lambda}\right)e^{-\frac{r}{\lambda}} \tag{26}$$

Substituting Eqs. (12), (13), (14) and (26) and then into (10) after a little algebra and simplification we obtain the following equation that gives the rate of change of the Tisserand parameter as a function of the eccentric anomaly E to be:

$$\frac{dT}{dE} = -GM\alpha\left[\frac{2eA_0}{n^2a^2} - \frac{B_0(1-e^2)}{n^2a^3}\right]\left[\frac{\sin E}{(1-e\cos E)^2}\left(1 + \frac{a(1-e\cos E)}{\lambda}\right)e^{-\frac{a(1-e\cos E)}{\lambda}}\right], \tag{27}$$

where:

$$A_0 = \left(\frac{a_J}{a^2} + \cos i\sqrt{\frac{(1-e^2)}{a_Ja}}\right) \tag{28}$$

$$B_0 = \frac{2ea\cos i}{\sqrt{a_Ja(1-e^2)}} \tag{29}$$

To find the Yukawa effect correction in the Tisserand parameter we integrate Eq. (20) for a full revolution, and therefore we obtain that:

$$T_{final} = T_{ini} - GM\alpha\left[\frac{2eA_0}{n^2a^2} - \frac{B_0(1-e^2)}{n^2a^3}\right]\int_0^{2\pi}\left[\frac{\sin E}{(1-e\cos E)^2}\left(1 + \frac{a(1-e\cos E)}{\lambda}\right)e^{-\frac{a(1-e\cos E)}{\lambda}}\right]dE \tag{30}$$

Again, using the same transformation as before i.e. $1-e\cos E = u$ the integral has the same upper and lower limit and therefore by definition the integral in (32) is equal to zero and therefore we have that:

$$T_{final} = T_{ini} = \text{constant} \tag{31}$$

Next consider the following cases of a and λ. First consider the case $a = \lambda$. In this case Eq. (30) takes the form:

$$T_{final} = T_{ini} - GM\alpha \left[\frac{2eA_0}{n^2a^2} - \frac{B_0(1 - e^2)}{n^2a^3} \right] \int\limits_0^{2\pi} \left[\frac{\sin E}{(1 - e\cos E)^2}(2 - e\cos E)e^{-(1 - e\cos E)} \right] dE, \tag{32}$$

which under the same transformation given under Eq. (32) results again to the same integration limits and therefore the integral in Eq. (32) is again zero, and therefore

$$T_{final} = T_{init} = \text{constant} \tag{33}$$

5 Tisserand Criterion in Potentials of Higher *D* Dimensions

To approach such a question, it will be necessary to have an idea of what a gravitational force in higher dimensions might be. For that let us consider a point in a D-dimensional Euclidean space with coordinates $(x_1, x_2, x_3......x_D)$, it's true that $\left(x_1^2 + x_2^2 + x_3^2.... + x_{D+1}^2\right) = R^2$ and where R is the radius of the hypersphere. For such a hypersphere the volume is given by (Rabinowitz 2001), where $\Gamma(D/2)$ is the gamma function of the indicated argument to be:

$$V_{D-1}(r) = \frac{(2\pi)^{D/2}r^{(D-1)}}{\Gamma\left(\frac{D}{2}\right)}, \tag{34}$$

Similarly, the D dimensional space gravitational force is given by (ibid 2001):

$$F_D(r) = -\frac{2\pi G_N Mm}{\pi^{D/2}r^{D-1}}\Gamma(D/2) \tag{35}$$

As a first example of higher dimension potential let us consider the $D=4$ case. Therefore, the radial acceleration or force per unit mass can be written as function of the eccentric anomaly takes the form:

$$R_D(r) = -\frac{4\pi G_4 M}{\pi r^3} = -\frac{4\pi G_4 M}{\pi a^3 (1 - e\cos E)^3} \tag{36}$$

where the gravitational constant G_4 is model depended if $D>3$ (Rabinowitz 2001). Therefore Eq. (10) can be now written as:

$$\frac{dT_c}{dE} = \left(-\frac{4\pi G_4 M}{\pi a^3 n}\right)\left(\frac{\sin E\sqrt{1 - e^2}}{(1 - e\cos E)^3}\right)\left[A_0\left(\frac{2e}{n\sqrt{1 - e^2}}\right) - B_0\left(\frac{\sqrt{1 - e^2}}{na}\right)\right] \tag{37}$$

Integrating over a full rotation we must calculate the integral:

$$\int_0^{2\pi} \frac{\sin E}{(1 - e \cos E)^3} dE = 0, \tag{38}$$

And therefore

$$T_{final} = T_{init} = \text{constant} \tag{39}$$

In the general D dimensional case we have that the radial acceleration per unit mass R_D takes the form

$$R_D(r) = -\frac{2\pi G_N M}{\pi^{D/2} r^{D-1}} \Gamma(D/2) = \frac{2\pi G_D M \Gamma(D/2)}{\pi^{D/2} a^{D-1} (1 - e \cos E)^{D-1}} \tag{40}$$

Using Eq. (4) Eq. (10) as a function of eccentric anomaly takes the form:

$$\frac{dT_c}{dE} = \left[-A_0 \left(\frac{4 e G_D M \pi^{\left(\frac{2-D}{2}\right)} \Gamma(D/2)}{n^2 a^{D-1}} \right) + B_0 \left(\frac{2 G_D M \pi^{\left(\frac{2-D}{2}\right)} (1 - e^2) \Gamma(D/2)}{n^2 a^D} \right) \right] \left(\frac{\sin E}{(1 - e \cos E)^{D-1}} \right) \tag{41}$$

Therefore, integrating over one revolution we have the following integral:

$$I_0 = \int_0^{2\pi} \frac{\sin E}{(1 - e \cos E)^{D-1}} dE = 0 \tag{42}$$

and therefore, the final Tisserand parameter after one revolution becomes:

$$T_{final} = T_{init} - \left[-A_0 \left(\frac{4 e G_D M \pi^{\left(\frac{2-D}{2}\right)} \Gamma(D/2)}{n^2 a^{D-1}} \right) + B_0 \left(\frac{2 G_D M \pi^{\left(\frac{2-D}{2}\right)} (1 - e^2) \Gamma(D/2)}{n^2 a^D} \right) \right] I_0 \tag{43}$$

And therefore

$$T_{(ini)_D} = T_{(ini)_D} = \text{constant} \tag{44}$$

At this point we say that since the dimensionality D must be an integer number even or odd the integral in Eq. (42) is equal to zero.

6 Tisserand Parameter in Fractal Dimensionality

Recent theoretical research in relation to various fields of physics for example superstrings (West 2012), and loop quantum gravity (Rovelli 2004) point out in the direction that higher dimensions and fractal geometry could be used to describe not just quantum mechanics but also relativity. Moreover, efforts in establishing physics beyond the standard model has also indicated the need of extra dimensions. Next, we will try to shed some light in explaining the concept of *fractal space–time* and for its mathematical description the reader could refer to Nottale, (1995). At this point we say that a fractal space–time theory it's not yet completed when compared to other theories such as special and general relativity and quantum

mechanics. Recent theories of quantum gravity space–time have a fractal structures. At Planck scales the theory predicts a two-dimensional space–time which eventually evolves into a four dimensional one at later times in the evolution of the universe. This is an effort of "trying to understand how a gravitation space with fractional dimensions couples with gravitation" (Helleman, 2006). Next, let us briefly mention how a fractal space–time can be represented mathematically. First, consider a small distance differential dX^i of a no differentiable 4-coordinates along one of the geodesics lines. Following Nottale (1996) we can decompose dX^i in terms of its mean, $< dX^i > = dx^i$ and a fluctuation respective to the mean, $d\xi^i$(such that $<d\xi^i> = 0$ by definition) and therefore we can write that:

$$dX^i = dx^i + d\xi^i \tag{45}$$

In this definition, the variables dx^i generalizes the classical variables, and $d\xi^i$ describe the new, non-classical, fractal behaviour (ibid 1996). Next according to the laws of fractal geometry (Mehaute 1990) this type of behaviour depends on the fractal dimension D according to the relation below:

$$d\xi = dt^{\frac{1}{D}}, \tag{46}$$

where D is the dimensionality of the fractal space and an existing number of different fractal dimensions in the literature (Falconer 1990). To estimate the fractal dimension, we use the definition (Hanan and Radu 2007)

$$d = \lim \frac{\ln(N(\varepsilon))}{\ln(1/\varepsilon)} \tag{47}$$

when $\varepsilon \to 0$, where $N(\varepsilon)$ is the minimal number of boxes of size ε needed to cover the fractal set. In practice one estimates d the fractal dimensionality. In this work we assume an orbiting comet with aphelion pass Jupiter distance. Let now assume the radial distance of the comet from the sun in AU be given by:

$$r_{AU} = r_0 + \alpha_0 N^D, \tag{48}$$

where r_0 is the cometary perihelion distance in AU and $\alpha_0 = \langle a_{per_i} \rangle$ in AU and D is fractal dimension, and N is the number of comets. We can think of the solar system as a system/structure that has fractal nature, which also exhibits scaling properties. If this proves true it will be a great help in understanding the origin of the solar system. Next, writing that the radial distance in terms of the eccentric anomaly E using Eq. (14) and equating to Eq. (48) solving for the fractal dimensionality we obtain that:

$$D = \frac{\ln\left[\frac{a(1-e\cos E)-r_0}{\alpha_0}\right]}{\ln(N)}, \tag{49}$$

Using Eq. (49) we can write Eq. (42) in the following way:

$$I_0 = \int_0^{2\pi} \frac{\sin E}{(1 - e\cos E)^{\xi(\varepsilon - \gamma\cos E)}} dE, \tag{50}$$

where $\alpha = \frac{a}{N}$, $\beta = \frac{r_0}{N}$, $\gamma = \frac{ae}{N}$ and $\varepsilon = \alpha - \beta = \frac{a - r_0}{N}$. Again, making the transformation $u = (1 - e\cos E)$ we obtain the following integral

$$I_0 = \int\limits_{1-e}^{1-e} \frac{du}{u^{\xi \ln\left(\varepsilon - \frac{\zeta}{e}(1-u)\right)}} = 0 \tag{51}$$

Therefore, we conclude that in even in D dimensional space where D is a fractal dimension the Tisserand parameter remains constant.

7 Tisserand Parameter and Orbit Quantization

To examine the invariability of Tisserand parameter to a quantized orbit let as use the result given in Rabinowitz (2001) in which the author considers quantized non-relativistic gravitational orbits in a D-space, analogous to electrostatic atomic orbitals (ibid 2001). Moreover, the author proceed by saying that ordinary matter does not have a density that is high enough to make orbits like this possible. Using a Bohr-Somerfield condition the author derives that the orbital radius around a primary body of mass M is given by:

$$r_n = \left[\frac{n\hbar}{m\left(2G_D M\, \Gamma(D/2)\right)^{1/2}} \right]^{\frac{2}{(4-D)}} \tag{52}$$

Equating Eq. (52) with the radial vector Eq. (12) we have the following equation:

$$a_n(1 - e\cos E) = \left[\frac{n\hbar}{m\left(2G_D M\, \Gamma(D/2)\right)^{1/2}} \right]^{\frac{2}{(4-D)}}, \tag{53}$$

solving for a_n we obtain the equation:

$$a_n = \frac{n\hbar\pi^{\left(\frac{D}{4} - \frac{1}{2}\right)} 2^{\frac{1}{(D-4)}} \left[m\left(G_D M\, \Gamma(D/2)\right) \right]^{\frac{2}{(D-4)}}}{(1 - e\cos E)} \tag{54}$$

Next assuming an orbiting comet/ planet for which the semi-major axes is quantized according to (54) and substituting in Tisserand parameter equation after some simplification we obtain that:

$$T = \frac{\left(1 - e_c \cos E_c\right)}{\left(1 - e_J \cos E_J\right)} + 2\cos i \sqrt{\left(1 - e_c^2\right) \frac{\left(1 - e_J \cos E_J\right)}{\left(1 - e_c \cos E_c\right)}} \tag{55}$$

Looking at Eq. (56) we realize that for given values of the comet/planet eccentricities e_p, e_c and eccentric anomalies E_p, E_c and cometary inclination i this equation is just a constant, therefore it does not change.

Next, we will continue in deriving analytical expressions with the help of which we can obtain the dependence of Tisserand's parameter on the semi major axis and the eccentricity of the orbit. Thus, using Eq. (3) and multiplying through by dt we obtain:

$$dT_c = A_0 da - B_0 de, \tag{56}$$

dividing Eq. (56) both by da we obtain:

$$\frac{\mathrm{d}T_c}{\mathrm{d}a} = A_0 - B_0 \frac{\mathrm{d}e}{\mathrm{d}a}, \tag{57}$$

similarly, w. r. t to eccentricity we obtain the following equation:

$$\frac{\mathrm{d}T_c}{\mathrm{d}e} = A_0 \frac{\mathrm{d}a}{\mathrm{d}e} - B_0, \tag{58}$$

where A_0 and B_0 are given by Eqs. (28) and (29) and the fact that

$$\frac{\mathrm{d}a}{\mathrm{d}e} = \frac{2ea}{\left(1 - e^2\right)} \tag{59}$$

$$\frac{\mathrm{d}e}{\mathrm{d}a} = \frac{\left(1 - e^2\right)}{2ea} \tag{60}$$

Using Eqs. (28), (29), 59, and (60) Eqs. (58) and (59) become:

$$\frac{\mathrm{d}T}{\mathrm{d}a} = \frac{a_J}{a^2} \tag{61}$$

$$\frac{\mathrm{d}T}{\mathrm{d}e} = \frac{2ea_J}{a\left(1 - e^2\right)} \tag{62}$$

and solving the differential Eq. (61) subjected to the initial condition $T\left(a_0\right) = T_{init}$ we obtain the following solution:

$$T(a)_{fin} = T_{init} + a_J \left(\frac{1}{a_0} - \frac{1}{a} \right) \tag{63}$$

Similarly, integrating Eq. (62) subjected to $T\left(e_0\right) = T_{init}$ we obtain:

$$T(e)_{fin} = T_{init} + \frac{2a_J}{a} \ln \left(\frac{1 - e_0^2}{1 - e^2} \right)^{1/2} \tag{64}$$

If $T(a)_{fin} = T_{init}$ then $\Delta T = 0$, using Eq. (64) this is possible if

$$a_J \left(\frac{1}{a_0} - \frac{1}{a} \right) = 0, \tag{65}$$

and

$$\frac{2a_J}{a} \ln \left(\frac{1 - e_0^2}{1 - e^2} \right)^{1/2} = 0, \tag{66}$$

Which from Eq. (65) and (66) implies that $a_0 = a$ and from Eq. (57) $a \to \infty$ or $e_0 = e$.

8 Tisserand Parameter in a Non-Singular and Quantum Correction to the Gravitational Potential

A non-singular gravitational potential can be represented by the following mathematical formula (Haranas and Pagiatakis 2010; Williams 1997, and 2001) of the following form:

$$V(r) = -\frac{GM}{r} e^{-\frac{\lambda}{r}}, \tag{67}$$

and the constant $\lambda << r$ is defined as follows:

$$\lambda = \frac{GM}{c^2}, \tag{68}$$

where c is the speed of light, G is Newton's gravitational constant, M_p is the mass of the primary body, r is the radial distance of the secondary from the center of the primary body. We can easily see that this potential its almost identical to the Yukawa potential, with the only exception that the Yukawa potential scales as $e^{-r/\lambda}$ the non-singular potential scales as $e^{-\lambda/r}$. For radial distances greater than λ it takes the familiar $1/r$ form. If $r=0$ the potential is zero due to the overriding effect of the exponential. In the case of this potential the radial component of the acceleration becomes:

$$R_{ns}(r) = -\frac{GM}{r}\left(1 - \frac{\lambda}{r}\right)e^{-\frac{\lambda}{r}} = -\frac{GM}{a(1 - e\cos E)}\left(1 - \frac{\lambda}{a(1 - e\cos E)}\right)e^{-\frac{\lambda}{a(1 - e\cos E)}}, \tag{69}$$

And therefore the equation of the rate of change of the Tisserand parameter with respect to the eccentric anomaly E becomes:

$$\frac{dT}{dE} = -GM\left[\frac{2eA_0}{n^2a} - \frac{B_0(1 - e^2)}{n^2a^3}\right]\left[\sin E\left(1 - \frac{\lambda}{a(1 - e\cos E)}\right)e^{-\frac{\lambda}{a(1 - e\cos E)}}\right] \tag{70}$$

Integrating we have

$$T_{fin} = T_{ini} - \int_0^{2\pi} GM\left[\frac{2eA_0}{n^2a} - \frac{B_0(1 - e^2)}{n^2a^3}\right]\left[\sin E\left(1 - \frac{\lambda}{a(1 - e\cos E)}\right)e^{-\frac{\lambda}{a(1 - e\cos E)}}\right], \tag{71}$$

$$T_{fin} = T_{ini} - \left[\frac{(1 - e\cos E)e^{-\frac{\lambda}{a(1 - e\cos E)}}}{e} + \frac{2\lambda}{ae}Ei\left(-\frac{\lambda}{a(1 - e\cos E)}\right)\right]_0^{2\pi} = 0, \tag{72}$$

and therefore

$$T_{fin} = T_{ini} = constant. \tag{73}$$

In the case of circular orbits Eq. (71) is equal to

$$T_{fin} = T_{ini} + \int_0^{2\pi} GM\left[\frac{B_0}{n^2a^3}\right]\left[\sin E\left(1 - \frac{\lambda}{a}\right)e^{-\frac{\lambda}{a}}\right]dE = 0, \tag{74}$$

And again

$$T_{fin} = T_{ini} = constant. \tag{75}$$

Finally in the case where $\lambda = a$, again the Tisserand parameter remains constant.

The Newtonian potential energy that is usually describes the motion of two bodies of mass M_p and m which are separated by a distance r:

$$V_p(r) = -\frac{GM_p}{r}, \tag{76}$$

where G is the Newtonian constant of gravitation. This is an approximately valid potential (e. g., Donoghue 1994). In the case of large masses or large velocities, General Relativity theory predicts that relativistic corrections exist, which can be calculated and also verified experimentally (e. g., Bjorken and Drell 1964). Similarly, in the microscopic distance domain, we could expect that Quantum Mechanics predicts a correction to the gravitational potential in similar way that corrections of Quantum Electrodynamics lead to a modification of the Coulomb interaction (t'Hooft and Veltman 1974). Even though General Relativity constitutes a well-defined classical theory, it is not possible yet to combine GR with Quantum Mechanics to create a satisfactory theory of Quantum Gravity. In reference to Hamber and Liu (1995) and Haranas and Mioc (2009), and taking into account that $M_p >> m$ and following Haranas et al. (2015) the corrected potential energy valid to order G^2 is given by:

$$V(r) = -\frac{GM_p m}{r} \left(1 - \frac{GM_p}{2c^2 r} - \frac{122 G\hbar}{15\pi c^3 r^3} \right), \tag{77}$$

And therefore the radial acceleration per unit mass is:

$$R_{qu}(r) = -\frac{\partial V_{qu}(r)}{\partial r} = \frac{122 G^2 M_p \hbar}{15\pi c^3 r^4} = \frac{122 GM_p \ell_{pl}^2}{5\pi r^4}, \tag{78}$$

where $\ell_{pl}^2 = \frac{G\hbar}{c^3}$ is the Planck length $= 1.616 \times 10^{-35}$ m, and therefore we have that:

$$\frac{dT}{dE} = \frac{GM_p \ell_p^2}{5\pi n^2 a^4} \left(244 e A_0 - \frac{122 B_0}{a} \left(1 - e^2\right) \right) \left(\frac{\sin E}{(1 - e \cos E)^4} \right) \tag{79}$$

Integrating over a full revolution we obtain:

$$T_{fin} = T_{ini} + \frac{GM_p \ell_p^2}{5\pi n^2 a^4} \left(244 e A_0 - \frac{122 B_0}{a} \left(1 - e^2\right) \right) \int_0^{2\pi} \frac{\sin E}{(1 - e \cos E)^4} = 0 \tag{80}$$

The quantum correction to the gravitational potential leaves the Tisserand parameter invariant. Finally, in the case of a Newtonian potential $V(r) = -GM/r$ we obtain the following equation:

$$\frac{dT}{dE} = \frac{GM_p \sin E}{n^2 a^2 (1 - e \cos E)^2} \left(2e A_0 + \frac{B_0}{a} \left(1 - e^2\right) \right), \tag{81}$$

Integrating over one revolution the integral involving the trigonometric terms is again equal to zero and therefore the Tisserand parameter remains constant again.

9 Discussion and Numerical Results

Consider Jupiter like comets with inclinations $i \leq 30°$ periods in the range 3–10 years and eccentricities in the range $0.5 \leq e \leq 0.7$ (Cole and Woolfson, 2013). In this contribution more exact values of the orbital elements of the comets *Tempel*-2, *Grigg-Skjellerup, Giacobini-Zinner* (ibid 2013) are used as they are given in (https://ssd. jpl. nasa. gov/tools/ sbdb_lookup. html#/). In Table 1 we tabulate the orbital elements used in our numerical calculation. We use the JPL-NASA results for the semimajor axes given in Table 1 and we assume that these values have been calculated using a Newtonian potential. In Table 2 we calculate the Tisserand parameters of the three comets and we find that they are in the range $2.46518 \leq T_{JF} \leq 2.96445$. In Table 3 we calculate the encounter velocities of the three Jupiter family comets. The velocities appear to be kind of low something that agrees with what has been said in a paper by Tancredi and Lindgren (1991) where the authors find that Jupiter family comets tend to have low encounter velocities at the encounter with Jupiter where their heliocentric orbital velocities at the moment of encounter are similar to the velocity of Jupiter.

It is known that comets with $T \leq 3$ corresponds to very slow comets with further implies a very strong Jupiter encounter. On the other hand, objects with $T > 3$ cannot cross Jupiter's orbit in the circular restricted case. Therefore, the comets can e bconfined either to totally exterior or interior orbits (Duncan 2008). According to Levison (1996), a significant category is based on the Tisserand parameter. In this classification comets with $T > 2$ are called ecliptic comet because of their small inclinations. Similarly, comets for which the following relation holds i.e. $2 < T < 3$ are associated with Jupiter-crossing orbits that are dynamically dominated by Jupiter (ibid 1996). Comets with $T < 2$ it is believed they originate in the Oort cloud (Oort 1950) are designated nearly isotropic comets (NIC). In the case of Jupiter family comets, the relative velocity between the comet and Jupiter is given by the relation (Carusi et al. 1995)

$$v_{rel_{com}} = v_{Jup}\sqrt{3 - T} = v_{Jup}\left[3 - \left(\frac{a_J}{a} + 2\cos i\sqrt{\frac{a(1 - e^2)}{a_J}}\right)\right]^{1/2}, \qquad (82)$$

where v_{Jup} is Jupiter's velocity around the sun taken to be as the mean orbital velocity of Jupiter to be $v_{Jup} = 13.0697$ km/s (Vallado, 2001) and a_J is approximately constant, and T is the Tisserand parameter. Therefore the acceleration of the comet relative to Jupiter becomes:

$$a_c = \frac{dv_c}{dt} = \frac{\left(\frac{2a_J}{a^2} + \cos i\sqrt{\frac{(1 - e^2)}{aa_J}}\right)\frac{da}{dt} - \frac{2ae\cos i}{\sqrt{aa_J(1 - e^2)}}\frac{de}{dt} + 2\sin i\sqrt{\frac{a(1 - e^2)}{a_J}}\frac{di}{dt}}{2\left[3 - \frac{a_J}{a^2} - 2\cos i\sqrt{\frac{a(1 - e^2)}{a_J}}\right]}, \qquad (83)$$

which in the case of circular orbits $e = 0$ becomes:

$$a_c = \frac{dv_c}{dt} = \frac{\left(\frac{2a_J}{a^2} + \frac{\cos i}{\sqrt{aa_J}}\right)\frac{da}{dt} + 2\sin i\sqrt{\frac{a}{a_J}}\frac{di}{dt}}{2\left[3 - \frac{a_J}{a^2} - 2\cos i\sqrt{\frac{a}{a_J}}\right]} \qquad (84)$$

Table 1 Orbital elements of the three Jupiter family comets used in this paper

Jupiter family comets	Orbital eccentricity e	Orbital inclination $[i°]$	Semi-major axis a [AU]	Perihelion distance a_p [AU]
Temle-2	0.5362602835158699	12.02539399414482	3.065339291995363	1.42151974197394
Grigg-Skjellerup	0.6330527671345312	22.35649066304651	3.043315833693677	1.116736323909562
Giacobinni-Zinner	0.7104667848114644	32.00303376160798	3.500440355594361	1.013493750730936

Similarly, if we consider the velocity of Jupiter to also vary with time the acceleration expression becomes:

$$a_c = v_J Q_0 + \left(\frac{v_c}{v_J}\right)\frac{dv_J}{dt}, \tag{85}$$

and for circular orbits Eq. (84) becomes:

$$a_c = v_J Q_0(e = 0) + \left(\frac{v_c(e = 0)}{v_J}\right)\frac{dv_J}{dt} \tag{86}$$

where Q_0 is given by:

$$Q_0 = \left(\frac{2a_J}{a^2} + \cos i\sqrt{\frac{(1 - e^2)}{aa_J}}\right)\frac{da}{dt} - \frac{2ae\cos i}{\sqrt{aa_J(1 - e^2)}}\frac{de}{dt} + 2\sin i\sqrt{\frac{a(1 - e^2)}{a_J}}\frac{di}{dt} \tag{87}$$

Using a mean orbital velocity of Jupiter to be $v_{Jup=}$ 13. 0697 km/s (Vallado 2001) to tabulate the relative velocities of the three comets relative Jupiter comets to be:

Next, we try to write a fractal equation for the radius of the cometary orbits and calculate the fractal orbital dimension D. We use Eqs. (48) and (12) where r_0 is the perihelion, e the orbital eccentricity, E is the eccentric anomaly, a the semimajor axis, and $\alpha_0 = \langle a_{p_i}\rangle = 1.18392$ AU or the average of the perihelia distances,

$$D = \frac{\ln\left[\frac{a(1 - e\cos E) - r_{0_i}}{\alpha_0}\right]}{\ln 3} = \frac{\ln\left[\frac{a(1 - e\cos E) - r_{p_i}}{\langle a_{p_i}\rangle}\right]}{\ln 3} \tag{88}$$

And therefore we obtain:

$$1.1425197419594 + 1.18392 \times 3^D = 3.065339291995363(1 - 0.5362602835158699\cos E) \tag{89}$$

$$1.116736323909562 + 1.18392 \times 3^D = 3.043315833693677(1 - 0.6330527671345312\cos E) \tag{90}$$

$$1.013493750730936 + 1.18392 \times 3^D = 3.500440355594361(1 - 0.710466784811464412\cos E) \tag{91}$$

Solving the above equations for the fractal dimension D of each come we obtain that:

$$D_{Temp-2} = \frac{\ln\left[\frac{1.42151974197594 + 3.065339291995363(1 - 0.5362602835158699\cos E)}{1.18392}\right]}{\ln 3} \tag{92}$$

Table 2 For the three Jupiter family comets of known orbital elements we tabulate the Tisserand parameters

Orbital eccentricity (e)	Tisserand parameter(T)
Temle-2	2.96445
Grigg-Skjellrup	2.80450
Giacobinni-Zinner	2.44652

Table 3 Relative velocities of comets with respect to Jupiter

Jupiter comets	Comet encounter velocityv_{en} [km/s]
Temle-2	2.46247
Grigg-Skjellrup	5.77457
Giacobinni-Zinner	9.55096

$$D_{Gri-Skj} = \frac{\ln\left[\frac{1.116736323909562 + 3.043315833693677(1 - 0.6330527671345312\cos E)}{1.18392}\right]}{\ln 3} \tag{93}$$

$$D_{Gia-Zin} = \frac{\ln\left[\frac{1.013493750730936 + 3.500440355594361(1 - 0.7104667848114644\cos E)}{1.18392}\right]}{\ln 3} \tag{94}$$

In Fig. 1 Eqs. (92) (93) (94) represent the change of the fractal dimension of the three Jupiter family comets in a full orbital revolution as a function of the eccentric anomaly namely Tempel-2 (blue), Grigg-Skjelderup (magenta), Giacobini-Zinner (yellow). The value of the Tissearand parameter is different for each comet and varies periodically as a function of the eccentric anomaly E of the cometary orbit. The peak value corresponds to the eccentric anomaly at 180^0. Moreover, we find that around the orbit the comets Tempel-2 (blue), Giacobini-Zinner (yellow) share a common dimensionality value at a certain range of eccentric anomaly namely which can be obtained from the graph by reading the coordinates at the points using the Mathematica software function. For example, for the comets Tempel-2/Giacobini-Zinner and in the left graph point of intersection is bounded between the following values eccentric anomaly $E = 88.\ 04°\ D(E) = 1.\ 248$ and $E = 98.\ 52°$ $D(E) = 1.\ 315$ and in the right intersection of the graph point we obtain that.

$E = 272.\ 1°\ D(E) = 1.\ 247$ and $E = 260.\ 4°\ D(E) = 1.\ 318$. Similarly in Fig. 2 we plot the cometary interaction velocity with Jupiter as a function of the orbital eccentric anomaly E of the three Jupiter family comets given above. Our graph resembles that of Carusi et al. (1995) in the domain of lower values of cometary interaction velocities. The graph demonstrates that the velocity of the comet periodically varies with the eccentric anomaly of the comet, having a maximum velocity value at aphelion, which in the case of these three comets being close to Jupiter and Jupiter's gravitational attraction is greater than that of the sun. Finally, in Fig. 3 we plot the interaction velocity versus values of the Tisserand parameters in the range that also includes the calculated Tisserand parameters of the three comets used in this contribution. We find that higher Tisserand parameters correspond to lower Jupiter encounter velocities.

Next let us consider the case of the variability of the fractal dimension let us consider the fractal dimension D to be a function of time and let us rewrite Eq. (48) in the following way:

$$r(t) = r_0(t) + \alpha_0 N^{D(t)} = a(t)(1 - e(t)) + \alpha_0 N^{D(t)} \tag{95}$$

Taking the time derivative of (96) and equating to $v_c = v_J\sqrt{3 - T}$ we obtain:

$$(1 - e)\frac{da}{dt} - a\frac{de}{dt} + \alpha_0 N^{D(t)} \ln N \frac{dD(t)}{dt} = v_J\sqrt{1 - T} \tag{96}$$

First assuming that $\frac{de}{dt} << 1$ in other words if there is a negligible effect on the eccentricity we obtain the following equation:

$$\frac{da(t)}{dt} + \frac{\alpha_0 \ln 3}{(1 - e)}N^{D(t)}\frac{dD(t)}{dt} = v_J\sqrt{1 - T} \tag{97}$$

For circular orbits $e=0$ and comets with Tisserand parameter $T=3$ we have the following equation:

$$\frac{da(t)}{dt} + \alpha_0 N^{D(t)} \ln 3\frac{dD(t)}{dt} = 0 \tag{98}$$

which can be written in the following way:

$$\frac{d}{dt}\left[a(t) + \alpha_0 N^{D(t)}\right] = 0 \tag{99}$$

Equation (93) subjected to the initial condition that $a(0)=a_0$ has a general solution of the form:
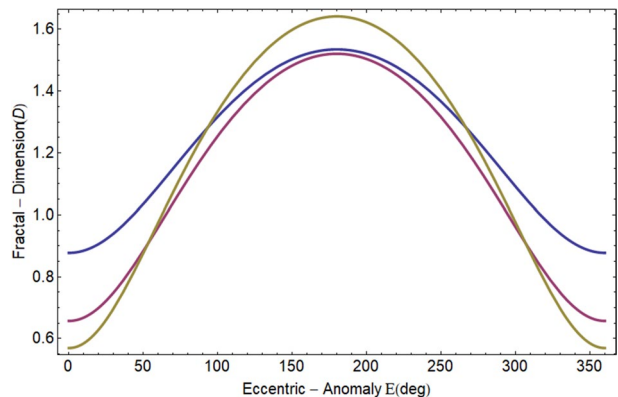
$$a(t) = c_0 - \alpha_0 N^{D(t)} \tag{100}$$

Using the initial condition that $a(0)=a_0$ we obtain that:

$$a(t) = a_0 + \alpha_0\left(N^{D(0)} - N^{D(t)}\right) \tag{101}$$

For comets that $T < 3$ and $e \neq 0$ we obtain that:

Fig. 1 In this figure we plot the fractal dimension D as a function of the eccentric anomaly E of the three Jupiter family comets namelyTampel-2 (blue), Grigg-Skjelderup (magenta), Giacobini-Zinner (yellow)

Fig. 2 In this figure we plot the cometary interaction velocity with Jupiter as a function of the eccentric anomaly E of the three Jupiter family comets namely Tampel-2 (blue), Grigg-Skjelderup (magenta), Giacobini-Zinner (yellow)
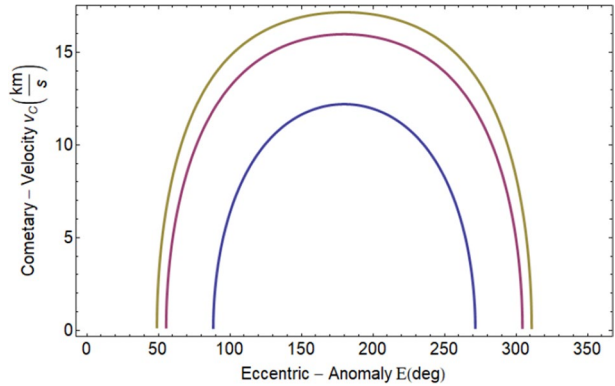
Fig. 3 Plot the comet closest approach velocity v_c as a function of the Tisserand parameter in the range $2.0 \leq T \leq 3.0$
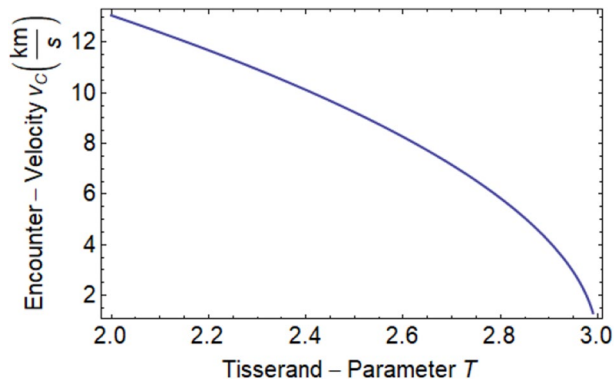
$$a(t) = a_0 - \frac{N^{D(t)}\alpha_0}{(1-e)} + v_J\left(\sqrt{3-T}\right)t \tag{102}$$

Substituting for D Eq. (49) using that $r_0(t) = r_p(t) = a(t)(1 - e(t))$ and finally D becomes:

$$D = \frac{1}{\ln N} \ln\left[\frac{ae(1 - \cos E)}{\alpha_0}\right], \tag{103}$$

$$\frac{da}{dt} + \frac{\alpha_0 a(1 - e\cos E)}{\left[1 + \alpha_0 e(1 - \cos E)\right]}\frac{de}{dt} + \frac{\alpha_0 e\sin E}{\left[1 + \alpha_0 e(1 - \cos E)\right]}\frac{dE}{dt} = \frac{v_J\sqrt{3-T}}{\left[1 + \alpha_0 e(1 - \cos E)\right]} \tag{104}$$

This is a more general equation for expressing the interaction velocity as function of the time rates of change of the orbital elements of the comet. Our work will follow up a paper soon.

10 Conclusions

The main goal in this contribution is the examination of the constancy of the Tisserand parameter under the potentials that various gravitational theories predict. For, for example theories that try to explain major difficulties in recent theory of gravitation, such as the problem of the flat rotation curves in spiral galaxies. Given that all these potentials are radially depended, we can calculate corresponding radial accelerations per unit mass and then the time rate of change of the basic orbital elements. Using Gauss' planetary equations, we derive an expression for the time rate of change of the Tisserand parameter as a function of the corresponding orbital time rates. Next, integrating over one orbital revolution we prove that the Tisserand parameter remains constant over one revolution for all the examined gravitational potentials. We also examine a D–dimensional gravitational potential resulting in a more generalized gravitational force in D dimensions and in the case of a $D = 4$-dimensional space. We find that in a four-dimensional space gravitational force the Tisserand parameter remains unchanged in one orbital revolution of the comet. Moreover, a fractal dimensional scenario is introduced which results from the effort in the bibliography to establish a physical understanding beyond the standard model. The radial distance of the comets is expressed of the fractal dimension D, which is also expressed as function as a function of the orbital elements of the comet. In the case of a quantized orbit the Tisserand parameter also remains unchanged. Finally, considering a time varying fractal dimension we derive and solve the time variability of the same- major axis of the comet as a function of a time variable fractal dimension.

References

A.C. Agnor, D.C. Lin, On the migration of jupiter and saturn: constraints from linear models of secular resonant coupling with the terrestrial planets. Astrophys. J. **745**(2), 143 (2011)

B. Bertotti, P. Farinella, D. Vokrouhlický, Physics of the solar system: dynamics and evolution space physics and spacetime structure, in *Astrophysics and Space Science Library*. (Kluwer Academic Publications, 2003), p.371

J.S. Binney, Tremaine, in *Galactic dynamics princeton series in astrophysics*. (Princeton University Press, 1987), p.590

J.D. Bjorken, S. Drell, *Relativistic quantum mechanics and relativistic quantum field theory* (McGraw-Hill, New York, 1964)

W.F. Bottke, A. Morbidelli, R. Jedicke, T.S. Metcalfe, Debiased orbital and absolute magnitude distribution of the near-earth objects. Icarus **156**(2), 399–433 (2002)

A. Carusi, L. Kresak, G.B. Valscesshi, Conservation of tisserand parameters at close encounters of interplaneatry objects with jupiter. Earth Moon Planet. **68**, 71–94 (1995)

C. Corda, Int. J. Mod. Phys. A **23**(10), 1521–1535 (2008)

C. Corda, Interferometric detection of gravitational waves: the definite test for general relativity. Int. J. Mod. Phys. D **18**(14), 2275–2282 (2009)

J.F. Donoghue, General relativity as an effective field theory: The leading quantum corrections. Phys. Rev. **50**, 3874 (1994)

J.M. Duncan, Space Sci. Rev. **138**, 1–4 (2008)

K. Falconer, *Fractal geometry and its applications* (Wiley, Chichester, 1990)

E. Fischbach, G.T. Gillies, D.E. Krause, J.G. Schwan, C. Talmadge, Metrologia **29**, 213 (1992)

E. Fischbach, D. Sudarsky, A. Szafer, C. Talmadge, S.H. Aronson, Phys. Rev. Lett. **56**, 3 (1986)

C.H.A. George, M.M. Woolfson, *Planetary science the science of planets around stars*, 2nd edn. (CRC Press, 2013), p.143

G.A. Gurzadyan, *Theory of interplanetary flights* (Gordon and Breach Publishers, 1996)

H.W. Hamber, S. Liu, Phys. Lett. B **357**, 51 (1995)

W. Hanan, Eugen Radu Chaotic motion in multi-black hole spacetimes and holographic screens. Mod. Phys. Lett. A **22**, 399–406 (2007)

I. Haranas, V. Mioc, Rom. Astron. J. **19**(2), 153–166 (2009)

I.S. Haranas, S. Pagiatakis, Satellite motion in a non-singular gravitational potential. Astrophys Space Sci. **327**, 83–89 (2010). https://doi.org/10.1007/s10509-010-0274-5

I. Haranas, O. Ragos, Yukawa-type effects in satellites dynamics. Astrophys. Space Sci. **331**, 115 (2010)

I. Haranas, K. Cobbett, I. Gkigkitzis, A. Alexiou, E. Cavan, Modified Newtonian dynamics effects in a region dominated by dark matter and a cosmological constant Λ. Astrophys. Space Sci. **365**, 171 (2020)

I. Haranas, O. Ragos, I. Gkigkitzis, I. Kotsireas, Quantum and post-Newtonian effects in the anomalistic period and the mean motion of celestial bodies. Astrophys. Space Sci. **358**, 1–8 (2015)

H.H. Hsieh, N. Haghighipur, Potential jupiter-family comet contamination of the main asteroid belt. Icarus **277**, 19–38 (2016)

L. Iorio, Phys. Lett. A **298**(5–6), 315 (2002)

L. Iorio, J. High Energy Phys. **10**, 041 (2007)

L. Iorio, Editorial for the special issue 100 years of chronogeometro-dynamics: the status of the Einstein's theory of gravitation in its centennial year. Universe **1**(1), 38–81 (2015)

N.I. Kolosnitsyn, V.N. Melnikov, Gen. Relativ. Gravit. **36**(7), 1619 (2004)

A. Le Mehaute, Les Geometries Fractales, Herm`es, Paris (1990)

H.F. Levison, Completing the inventory of the solar system, in Astronomical Society of the Pacific Conference Proceedings, vol 107, pp. 173–191 (1996).

D.M. Lucchesi, Phys. Lett. A **318**, 234 (2003)

M. Milgrom, Astrophys. J. **83**, 270–365 (1983)

C.D. Murray, S.F. Dermott, *Solar system dynamics* (Cambridge University Press, 1999)

J.H. Oort, The structure of the cloud of comets surrounding the solar system and a hypothesis concerning its origin. Bull. Astron. Inst. Neth. **11**, 91–110 (1950)

E.V. Pitjeva, Study of the Mars Dynamics based on the Analysis of Observations of the Viking and Pathfinder Landers. Tr. Inst. Prikl. Astron. Ross. Akad. Nauk. **4**, 22–35 (1999)

E.V. Pitjeva, Bull. Am. Astron. Soc. **41**, 881 (2009)

M. Rabinowitz, n-Dimensional gravity: little black holes, dark matter, and ball lightning. Int. J. Theor. Phys. **40**, 875–901 (2001)

C. Rovelli, *Quantum Gravity* (Cambridge Press, Cambridge, 2004)

R.H. Sanders, E. Noordermeer, Mon. Not. R. Astron. Soc. **379**, 702 (2007)

G. t'Hooft, M. Veltman, Ann. Inst. Henri Poincaré A **20**, 69 (1974)

G. Tancredi, M. Lindgren, The vicinity of Jupiter: a region to look for comets, in *Asteroids comets meteors*. ed. by T. Dev (Lunar and Planetary Institute, Houston, 1991), pp.601–604

A.D. Vallado, *McClain fundamentals of astrodynamics and applications* (Space Technology Library, 2001), p.907

P. West, *Introduction to Strings and Branes* (Cambridge University Press, Cambridge, 2012)

P.E. Williams, Thermodynamic basis for the constancy of the speed of light. Mod. Phys. Lett. A **12**, 35 (1997)

P. Williams, Mechanical entropy and its implications. Entropy **3**, 76–115 (2001)

Authors and Affiliations

Ioannis Haranas[1] · Youssef M. Shehata[2] · Kristin Cobbett[2] · Ioannis Gkigkitzis[3] · Dimitrios Theodore Kalafatis[4] · Ryan Gauthier[2]

✉ Ioannis Haranas
iharanas@wlu.ca

Kristin Cobbett
cobb2390@mylaurier.ca

Ioannis Gkigkitzis
igkigkitzis@nvcc.edu

Dimitrios Theodore Kalafatis
dtkalafatis@gmail.com

Ryan Gauthier
gaut0700@mylaurier.ca

[1]   College of Arts and Sciences, American University of Iraq, Airport Road, Baghdad, Iraq

[2]   Department of Physics and Computer Science, Wilfrid Laurier University Science Building, 75 University Ave. W., Waterloo, ON N2L 3C5, Canada

[3]   Department of Mathematics, NOVA, 8333 Little River Turnpike, Annandale, VA 22003, USA

[4]   Cinco Ranch High School, Cinco Ranch Blvd Katy Texas, Texas 77494, USA